Inorg. Chem. **2008**, *47*, 8641−8651

Synthesis, X-Ray Crystal Structures, and Phosphate Ester Cleavage Properties of *bis*(2-Pyridylmethyl)amine Copper(II) Complexes with Guanidinium Pendant Groups

Matthew J. Belousoff,[†] Linda Tjioe,[†] Bim Graham,*[,‡] and Leone Spiccia*[,†]

School of Chemistry, Monash University, Clayton, Vic 3800, Australia, and Medicinal Chemistry and Drug Action, Monash Institute of Pharmaceutical Sciences, Monash University, Parkville, Vic 3052, Australia

Received March 6, 2008

Three new derivatives of *bis*(2-pyridylmethyl)amine (DPA) featuring ethylguanidinium (L^1), propylguanidinium (L^2), or butylguanidinium (L^3) pendant groups have been prepared by the reaction of *N*,*N*-*bis*(2-pyridylmethyl)alkane-α,ω-diamines with 1*H*-pyrazole-1-carboxamidine hydrochloride. The corresponding mononuclear copper(II) complexes were prepared by reacting the ligands with copper(II) nitrate and were isolated as $[Cu(LH^+)(OH_2)](ClO_4)_3 \cdot xNaClO_4 \cdot yH_2O$ (**C1**: L = L^1, $x = 2$, $y = 3$; **C2**: L = L^2, $x = 2$, $y = 4$; **C3**: L = L^3, $x = 1$, $y = 0$) following cation exchange purification. Recrystallization yielded crystals of composition $[Cu(LH^+)(X)](ClO_4)_3 \cdot X$ (**C1′**: L = L^1, X = MeOH; **C2′**: L = L^2, X = H_2O; **C3′**: L = L^3, X = H_2O), which were suitable for X-ray crystallography. The crystal structures of **C1′**, **C2′**, and **C3′** indicate that the DPA moieties of the ligands coordinate to the copper(II) centers in a meridional fashion, with a water or methanol molecule occupying the fourth basal position. Weakly bound perchlorate anions located in the axial positions complete the distorted octahedral coordination spheres. The noncoordinating, monoprotonated guanidinium groups project away from the Cu(II)−DPA units and are involved in extensive charge-assisted hydrogen-bonding interactions with cocrystallized water/methanol molecules and perchlorate anions within the crystal lattices. The copper(II) complexes were tested for their ability to promote the cleavage of two model phosphodiesters, *bis*(*p*-nitrophenyl)phosphate (BNPP) and uridine-3′-*p*-nitrophenylphosphate (UpNP), as well as supercoiled plasmid DNA (pBR 322). While the presence of the guanidine pendants was found to be detrimental to BNPP cleavage efficiency, the functionalized complexes were found to cleave plasmid DNA and, in some cases, the model ribose phosphate diester, UpNP, at a faster rate than the parent copper(II) complex of DPA.

Introduction

Reactions involving the formation or cleavage of phosphate ester linkages are ubiquitous in biochemistry and underpin many fundamental biological processes, such as cellular signaling and regulation; energy storage and production; and nucleic acid synthesis, degradation, and repair.[1] These reactions are invariably catalyzed by enzymes, since they otherwise occur at rates that are far too slow to sustain life. Nuclease enzymes, for example, accelerate cleavage of the highly stable phosphate diester linkages in nucleic acids by up to a factor of 10^{17},[2] which is essential for several basic cellular functions, including DNA repair, RNA maturation, and the degradation of "foreign" nucleic acids and host cell DNA following infection.

The past two decades have seen escalating interest in the design and synthesis of low-molecular-weight compounds that are able to mimic key structural or functional aspects of enzymes involved in phosphoryl group transfer or phosphate ester cleavage reactions. As well testing and expanding our understanding of how these enzymes work, this research has the potential to deliver new therapeutic agents and tools for molecular biology. A major focus has

* Authors to whom correspondence should be addressed. Fax: +61 3 9903 9582 (B.G.), +61 3 9905 4597 (L.S.). E-mail: bim.graham@vcp.monash.edu.au (B.G.), leone.spiccia@sci.monash.edu.au (L.S.).

† School of Chemistry.

‡ Monash Institute of Pharmaceutical Sciences.

(1) Lehninger, A. L.; Cox, M. M.; Nelson, D. L. *Lehninger Principles of Biochemistry*, 4th ed.; W. H. Freeman: New York, 2005.

(2) Williams, N. H.; Takasaki, B.; Wall, M.; Chin, J. *Acc. Chem. Res.* **1999**, *32*, 485–493.

10.1021/ic8004079 CCC: $40.75
Published on Web 08/28/2008

been the development of small, hydrolytically active transition metal complexes as models for nuclease or phosphatase enzymes containing one or more metal ions at their active sites.[3−13] These metal ions assist the catalytic cleavage of phosphate esters by (i) activating the substrate through metal coordination; (ii) providing metal-bound hydroxide, alkoxide, or oxide groups that serve as nucleophiles or bases; (iii) facilitating the departure of leaving groups; and (iv) stabilizing transition states. A wide range of metal complexes have been reported that can cleave a variety of phosphate esters, including RNA and DNA, *via* one or more of these mechanisms, and in some cases, catalytic turnover has been demonstrated.[13−15] While cleavage rates several orders of magnitude above background levels have been achieved with simple metal complexes, the remarkable catalytic efficiencies of the native enzymes have yet to be realized.

In the quest to generate cleavage agents with improved activity, a fairly recent development has been the structural elaboration of metal complexes to include auxiliary groups that complement the hydrolytic action of the metal ion(s). Inspiration for these designs has come from the enzymes themselves, which, in addition to metal ions, contain amino acid residues at their active sites that assist catalysis by activating the substrate, promoting protonation/deprotonation processes, as well as stabilizing transition states. A classic example of this is provided by the zinc-containing enzyme alkaline phosphatase (AP). A crystal structure of AP, isolated from *Escherichia coli* and cocrystallized with orthophosphate, shows the presence of an arginine residue within hydrogen-bonding distance of the zinc-bound phosphate (Figure 1), as well as a nearby serine residue.[16] The arginine's positively charged guanidine group is thought to assist with substrate activation and transition-state stabilization, while the serine residue provides the attacking nucleophile, leading to the formation of a phosphoseryl intermediate during AP's catalytic cycle.[16,17] Complexes have been developed that can mimic this *cooperativity* between the metal ions and amino acid residues. Koevari and Krämer,[18] for example, showed that a copper(II) complex of a ligand featuring an in-built, hydrogen-bonding amine pendant was able to hydrolyze a model phosphate ester 3000 times faster than an analogue without such a pendant group. Similarly, Anslyn and co-workers[19] reported that the introduction of guanidine groups into a zinc(II) complex enhanced the complex's ability to hydrolyze a diribonucleotide. A number of other complexes bearing amino, ammonium or guanidine groups that cleave model phosphate esters or plasmid DNA more rapidly than their nonfunctionalized counterparts have been reported since.[10,20−23] Several groups have also developed complexes featuring alcohol pendants that are able to promote the cleavage of various phosphate esters *via* nucleophilic attack of the alcohol/alkoxide pendants on metal-bond substrates.[24,25]

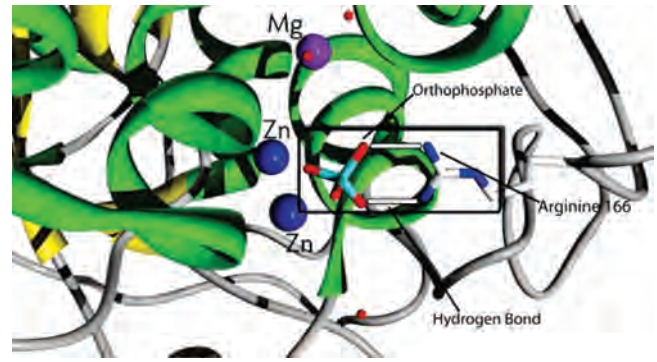

Figure 1. Detail of the X-ray crystal structure of the active site of *E. coli* alkaline phosphatase.[26] In the highlighted box is the cocrystallized phosphate, which is coordinated to two Zn(II) centers (bonds not shown for clarity) and hydrogen-bonded to an adjacent arginine residue. (Structure generated from PDB entry: 1ALK, using the UCSF Chimera Software Package[27]).

In this work, we extend the family of metal complexes with an in-built cationic hydrogen-bond donor. Our complexes feature ligands based on the well-known chelating agent *bis*(2-pyridylmethyl)amine (DPA). Early work by Chin and co-workers[28] demonstrated that copper(II) complexes of DPA derivatives greatly enhance the rate of transesterification of model phosphate diesters. This work has been followed up by a number of other research groups, who have shown that multinuclear complexes,[29−31] and complexes of different metals,[32] based on DPA ligands are able to hydrolyze a variety of

(3) Hegg, E. L.; Burstyn, J. N. *Coord. Chem. Rev.* **1998**, *173*, 133–165.
(4) Hegg, E. L.; Burstyn, J. N. *Inorg. Chem.* **1996**, *35*, 7474–7481.
(5) McCue, K. P.; Morrow, J. R. *Inorg. Chem.* **1999**, *38*, 6136–6142.
(6) Iranzo, O.; Richard, J. P.; Morrow, J. R. *Inorg. Chem.* **2004**, *43*, 1743–1750.
(7) Iranzo, O.; Richard, J. P.; Morrow, J. R.; Elmer, T. *Inorg. Chem.* **2003**, *42*, 7737–7746.
(8) Hegg, E. L.; Burstyn, J. N.; Deal, K. A.; Kiessling, L. L. *Inorg. Chem.* **1997**, *36*, 1715–1718.
(9) Deal, K. A.; Burstyn, J. N. *Inorg. Chem.* **1996**, *35*, 2792–2798.
(10) Mancin, F.; Tecilla, P. *New J. Chem.* **2007**, *31*, 800–817.
(11) Liu, C.; Wang, M.; Zhang, T.; Sun, H. *Coord. Chem. Rev.* **2004**, *248*, 147–168.
(12) Belousoff, M. J.; Duriska, M. B.; Graham, B.; Batten, S. R.; Moubaraki, B.; Murray, K. S.; Spiccia, L. *Inorg. Chem.* **2006**, *45*, 3746–3755.
(13) Fry, F.; Fischmann, A.; Belousoff, M. J.; Spiccia, L.; Brugger, J. *Inorg. Chem.* **2005**, *44*, 941–950.
(14) Scarso, A.; Scheffer, U.; Gobel, M.; Broxterman, Q. B.; Kaptein, B.; Formaggio, F.; Toniolo, C.; Scrimin, P. *Proc. Natl. Acad. Sci. U. S. A.* **2002**, *99*, 5144–5149.
(15) Deck, K. M.; Tseng, T. A.; Burstyn, J. N. *Inorg. Chem.* **2002**, 669–677.
(16) Kim, E. E.; Wyckoff, H. W. *J. Mol. Biol.* **1991**, *218*, 449–464.
(17) Coleman, J. E. *Annu. Rev. Biophys. Biomol. Struct.* **1992**, *21*, 441–483.
(18) Koevari, E.; Kräemer, R. *J. Am. Chem. Soc.* **1996**, *118*, 12704–12709.
(19) Ait-Haddou, H.; Sumaoka, J.; Wiskur, S. J.; Folmer-Andersen, J. F.; Anslyn, E. V. *Angew. Chem., Int. Ed.* **2002**, *41*, 4014–4016.
(20) Natale, D.; Mareque-Rivas, J. C. *Chem. Commun.* **2008**, 425–437.
(21) Sheng, X.; Lu, X.-M.; Chen, Y.-T.; Lu, G.-U.; Zhang, J.-J.; Shao, Y.; Liu, F.; Xu, Q. *Chem.—Eur. J.* **2007**, *13*, 9703–9712.
(22) Chen, X.; Wang, J.; Sun, S.; Fan, J.; Wu, S.; Liu, J.; Ma, S.; Zhang, L.; Peng, X. *Bioorg. Med. Chem. Lett.* **2008**, *18*, 109–113.
(23) An, Y.; Tong, M.-L.; Ji, L.-N.; Mao, Z.-W. *Dalton Trans.* **2006**, 2066–2071.
(24) Livieri, M.; Mancin, F.; Tonellato, U.; Chin, J. *Chem. Commun.* **2004**, 2862–2863.
(25) Zhang, Y.; Liang, H. C. *Inorg. Chem. Commun.* **2006**, *9*, 460–463.
(26) Kim, E. E.; Wyckoff, H. W. *J. Mol. Biol.* **1991**, *218*, 449.
(27) Pettersen, E. F.; Goddard, T. D.; Huang, C. C.; Couch, G. S.; Greenblatt, D. M.; Meng, E. C.; Ferrin, T. E. *J. Comput. Chem.* **2004**, *25*, 1605–1612.
(28) Wahnon, D.; Hynes, R. C.; Chin, J. *Chem. Commun.* **1994**, 1441–1442.

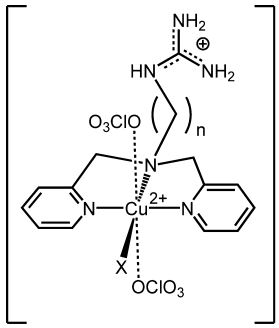

$(ClO_4).xNaClO_4.yH_2O.zMeOH$

C1: n = 2, X = H_2O, x = 2, y = 3, z = 0
C1': n = 2, X = MeOH, x = 0, y = 0, z = 1
C2: n = 3, X = H_2O, x = 2, y = 4, z = 0
C2': n = 3, X = H_2O, x = 0, y = 1, z = 0
C3: n = 4, X = H_2O, x = 1, y = 0, z = 0
C3': n = 4, X = H_2O, x = 0, y = 1, z = 0

Figure 2. Copper(II) complexes of *bis*(2-pyridylmethyl)amine (DPA) derivatives synthesized in this study.

phosphate esters, including activated phosphate esters, diribonucleotides, and plasmid DNA. The addition of hydroxyl or amino functionalities to simple DPA and *tris*(2-pyridylmethyl)amine complexes has also been investigated by the research groups of Mareque-Rivas, Williams and Chin and was found to result in enhanced cleavage activity.[24,33−35] Here, we have synthesized a new series of DPA-based ligands featuring guanidinium pendants, together with the corresponding copper(II) complexes (Figure 2). The ability of the complexes to promote the cleavage of three different phosphate diesters, namely, pBR 322 plasmid DNA, *bis*(*p*-nitrophenyl)phosphate (BNPP), and the activated RNA mimic uridine-3′-*p*-nitrophenylphosphate (UpNP), has also been investigated in order to gain some insight into the effect of the appended guanidinium groups on cleavage activity.

Experimental Section

Materials and Chemicals. Chemicals used in the synthesis were of reagent or analytical grade and were used as received. High-performance liquid chromatography grade chloroform and distilled H_2O were used throughout, and N,N-dimethylformamide (DMF) was dried over 4 Å sieves. DPA,[36] the *N*,*N*-*bis*(2-pyridylmethyl)-alkane-α,ω-diamines,[37] $[Cu(DPA)Cl_2]$,[38] $[Cu(tacn)Br_2]$,[39] $[Cu(Me_3tacn)(OH_2)_2]$-$(ClO_4)_2$,[10] and UpNP[40] were prepared according to published procedures. The pBR 322 plasmid DNA and agarose were purchased from Promega Corporation. *N*-[2-hydroxyethyl]piperazine-*N*′-[2-ethanesulfonic acid] (HEPES) and ethidium bromide (EB), bromophenol blue, glycerol, and ethylenediaminetetraacetic acid (EDTA) were used as received from commercial suppliers. MilliQ water used for DNA cleavage experiments was sterilized by autoclaving, and all reaction solutions were prepared according to standard sterile techniques.

Instrumentation and Methods. *Infrared spectra* were recorded as KBr disks using a Bruker Equinox FTIR spectrometer at 4.0 cm^{-1} resolution, fitted with an ATR platform. *Microanalytical* (C, H, and N) analyses were performed by Campbell Microanalytical Service, Otago, New Zealand. *^{1}H NMR and ^{13}C NMR spectra* were recorded at 25 °C in D_2O on a Bruker AC200, AM300, or DX400 spectrometer. Abbreviations used to describe the resonances for ^{1}H NMR spectra are s (singlet), d (doublet), t (triplet), and m (multiplet). *Low-resolution electrospray mass spectra* were obtained with a Micromass Platform II Quadrupole Mass Spectrometer fitted with an electrospray source. The capillary voltage was at 3.5 eV, and the cone voltage was at 35 V. *UV−vis−NIR spectra* were recorded on 0.01−10 mM solutions in quartz cuvettes using Varian Cary 3 or 5G spectrophotometers. *Cation exchange column chromatography* was performed using Sephadex SP-C25 columns (Na^+ form) with a 30 mm diameter. *Agarose gel electrophoresis* of plasmid DNA cleavage products was performed using a Biorad Mini-Protean 3 Electrophoresis Module. Bands were visualized by UV light irradiation, fluorescence-imaged using an AlphaImager, and photographed with a CCD camera. The photographed gels were analyzed with the aid of the program ImageQuaNT, version 4.1.

Caution! *Although no problems were encountered in this work, transition metal perchlorates are potentially explosive and should be prepared in small quantities and handled with care.*

Syntheses. *N*,*N*-*bis*(2-Pyridylmethyl)-*N*′-(carboxamidine)ethane-1,2-diamine Hydrochloride (L^1·HCl). To a solution of *N*,*N*-*bis*(2-pyridylmethyl)ethane-1,2-diamine (0.848 g, 3.50 mmol) in DMF (10 mL) was added 1*H*-pyrazole-1-carboxamidine hydrochloride (0.513 g, 3.50 mmol) and diisopropylamine (DIEA; 0.452 g, 3.50 mmol). The resulting solution was stirred overnight at room temperature. Diethyl ether (50 mL) was then added and the mixture cooled to 4 °C for 1 h, resulting in the separation of the crude product as a brown oil. The supernatant was decanted off and the oil extracted with ether (3 × 20 mL) and then acetone (3 × 20 mL), before being dried under a high vacuum for 4 h. Yield: 1.02 g, 90%. ^{1}H NMR (D_2O): δ 2.75 (t, 2H, J = 5.6 Hz, $NCH_2CH_2NHC(NH_2)_2$), 3.16 (t, 2H, J = 5.8 Hz, $NCH_2CH_2NHC(NH_2)_2$), 3.74 (s, 4H, pyridyl CH_2), 7.30 (m, 2H, pyridyl CH), 7.38 (d, 2H, J = 7.8 Hz, pyridyl CH), 7.77 (m, 2H, pyridyl CH), 8.38 (d, 2H, J = 5.1 Hz, pyridyl CH). ^{13}C NMR (D_2O): δ 33.33, 46.99, 53.91, 117.39, 118.74, 132.59, 141.87, 151.28. ESI-MS (*m*/*z*): 285.2 $[M + H]^+$ (100%).

***N*,*N*-*bis*(2-Pyridylmethyl)-*N*′-(carboxamidine)propane-1,3-diamine Hydrochloride (L^2·HCl).** The synthesis of L^2·HCl followed the method used to prepare L^1·HCl, with the following reagent quantities: *N*,*N*-*bis*(2-pyridylmethyl)propane-1,3-diamine (0.570 g, 2.22 mmol), 1*H*-pyrazole-1-carboxamidine hydrochloride (0.326 g, 2.22 mmol), and DIEA (0.287 g, 2.22 mmol). Yield: 0.653 g, 88%. ^{1}H NMR (D_2O): δ 1.75 (m, 2H, $NCH_2CH_2CH_2NHC(NH_2)_2$), 2.65 (t, 2H, J = 7.2 Hz, $NCH_2CH_2CH_2NHC(NH_2)_2$), 3.10 (t, 2H, J = 6.4 Hz, $NCH_2CH_2CH_2NHC(NH_2)_2$), 3.83 (s, 4H, pyridyl CH_2), 7.32 (m, 2H, pyridyl CH), 7.41 (d, 2H, J = 7.9 Hz, pyridyl CH), 7.79 (m, 2H, pyridyl CH), 8.41 (d, 2H, J = 5.9 Hz, pyridyl CH). ^{13}C

(29) Humphreys, K. J.; Karlin, K. D.; Rokita, S. E. *J. Am. Chem. Soc.* **2002**, *124*, 8055–8066.
(30) An, Y.; Liu, S.-Y.; Ji, L.-N.; Mao, Z.-W. *J. Inorg. Biochem.* **2006**, *100*, 1586–1593.
(31) Komiyama, M.; Kina, S.; Matsumura, K.; Sumaoka, J.; Tobey, S.; Lynch, V. M.; Anslyn, E. *J. Am. Chem. Soc.* **2002**, *124*, 13731–13736.
(32) Yashiro, M.; Ishikubo, A.; Komiyama, M. *Chem. Commun.* **1997**, 83–84.
(33) Young, M. J.; Wahnon, D.; Hynes, R. C.; Chin, J. *J. Am. Chem. Soc.* **1995**, *117*, 9441–9447.
(34) Feng, G.; Mareque-Rivas, J. C.; Torres Martin De Rosales, R.; Williams, N. H. *J. Am. Chem. Soc.* **2005**, *127*, 13470–13471.
(35) Feng, G.; Natale, D.; Prabaharan, R.; Mareque-Rivas, J. C.; Williams, N. H.; Zhang, Y.; Liang, H. C. *Inorg. Chem. Commun.* **2006**, *9*, 460–463.
(36) Incarvito, C.; Lam, M.; Rhatigan, B.; Rheingold, A. L.; Qin, C. J.; Gavrilova, A. L.; Bosnich, B. *Dalton Trans.* **2001**, 3478–3488.
(37) Matouzenko, G. S.; Bousseksou, A.; Lecocq, S.; van Koningsbruggen, P. J.; Perrin, M.; Kahn, O.; Collet, A. *Inorg. Chem.* **1997**, *36*, 5869–5879.
(38) Choi, K.-Y.; Ryu, H.; Sung, N.-D.; Suh, M. *J. Chem. Crystallogr.* **2003**, *33*, 947–950.
(39) Yang, R.; Zompa, L. J. *Inorg. Chem.* **1976**, *15*, 1499.
(40) Rishavy, M. A.; Hengge, A. C.; Cleland, W. W. *Bioorganic Chem.* **2000**, *28*, 283–292.

Table 1. Crystallography Collection and Refinement Data

crystal	C1′	C2′	C3′
empirical formula	$C_{17}H_{29}Cl_3CuN_6O_{14}$	$C_{16}H_{27}Cl_3CuN_6O_{14}$	$C_{17}H_{29}Cl_3CuN_6O_{14}$
M/g mol^{-1}	711.35	697.33	711.34
cryst syst	monoclinic	monoclinic	monoclinic
space group	$P2_1/n$	$P2_1/n$	$P2_1/c$
a/Å	19.190(2)	8.1297(10)	8.1767(8)
b/Å	7.3390(8)	14.3864(7)	15.9520(17)
c/Å	20.858(2)	22.7686(12)	20.829(2)
β/deg	111.742(6)	97.201(4)	98.166(6)
V/Å^3	2728.6(5)	2642.0(4)	2689.2(5)
Z	4	4	4
T/K	123(2)	123(2)	123(2)
λ/Å	0.71073	0.71073	0.71073
D_{alcdc}/g cm^{-3}	1.732	1.753	1.752
M(Mo Kα)/mm^{-1}	1.173	1.209	1.190
no. data measured	39832	13294	34383
unique data (R_{int})	9092 (0.308)	13294 (n/a)	6175 (0.0521)
observed data [I > 2(σ)I]	7959	12082	4926
final R1, wR2 (obsd data)	0.0555[a], 0.1380[b]	0.0636[a], 0.1788[b]	0.0725[a], 0.1438[b]
final R1, wR2 (all data)	0.0635, 0.1442	0.0698, 0.1823	0.0912, 0.1501
$\rho_{\mathrm{min}},\rho_{\mathrm{max}}/e$ Å^{-3}	−1.126, 1.635	−0.862, 1.050	−0.813, 0.722

[a] $R = \sum(|F_o| - |F_c|)/\sum|F_o|$. [b] $R' = [\sum w(|F_o| - |F_c|)^2/\sum F_o^2]^{1/2}$, where $w = [\sigma^2(F_o)]^{-1}$.

NMR (D_2O): δ 18.68, 32.96, 44.88, 53.46, 117.49, 118.83, 132.33, 142.24, 150.38. ESI-MS (m/z): 299.2 $[M + H]^+$ (100%).

***N,N-bis*(2-Pyridylmethyl)-*N*′-(carboxamidine)butane-1,4-diamine Hydrochloride (L^3·HCl).** This compound was prepared in the same manner as L^1·HCl using *N,N-bis*(2-pyridylmethyl)butane-1,4-diamine (0.500 g, 1.85 mmol), 1*H*-pyrazole-1-carboxamidine hydrochloride (0.271 g, 1.85 mmol), and DIEA (0.239 g, 1.85 mmol). Yield: 0.606 g, 94%. ^{1}H NMR (D_2O): δ 1.44, (m, 4H, $NCH_2CH_2CH_2CH_2NHC(NH_2)_2$), 2.53 (t, 2H, $J = 7.2$ Hz, $NCH_2CH_2CH_2CH_2NHC(NH_2)_2$), 3.01 (t, 2H, $J = 6.4$ Hz, $NCH_2CH_2CH_2CH_2NHC(NH_2)_2$), 3.75 (s, 4H, pyridyl CH_2), 7.27 (m, 2H, pyridyl CH), 7.36 (d, 2H, $J = 7.9$ Hz, pyridyl CH), 7.73 (m, 2H, pyridyl CH), 8.37 (d, 2H, $J = 5.0$ Hz, pyridyl CH). ^{13}C NMR (D_2O): δ 21.59, 24.66, 39.71, 52.61, 58.44, 122.27, 123.59, 137.02, 147.21, 155.54. ESI-MS (m/z): 313.2 $[M + H]^+$ (100%).

$[Cu(L^1H^+)(OH_2)](ClO_4)_3\cdot 2NaClO_4\cdot 3H_2O$ (C1) and $[Cu(L^1H^+)(MeOH)](ClO_4)_3\cdot MeOH$ (C1′). $Cu(NO_3)_2\cdot 3H_2O$ (0.513 g, 2.30 mmol) was dissolved in an aqueous solution (10 mL) of L^1·HCl (0.327 g, 1.00 mmol), resulting in a color change to dark blue. The solution was diluted to a volume of 2 L with water and then loaded onto a Sephadex (SP-C25) column. After it was washed with 0.2 M $NaClO_4$, a dark blue band corresponding to the complex was eluted with 0.5 M $NaClO_4$. The collected eluate was concentrated to ca. 50 mL using a rotary evaporator and then left to slowly evaporate in a crystallizing dish. After ca. 1 week, the dark blue needles of **1** that formed were filtered off, washed very quickly with ice-cold MeOH (2 mL), and air-dried. Yield: 0.289 g, 29.5%. Anal. calcd for $C_{15}H_{29}Cl_5CuN_6O_{24}Na_2$: C, 18.7; H, 3.0; N, 8.7%. Found: C, 18.7; H, 2.8; N, 8.6%. UV−vis (H_2O), λ_{max} (nm) [$\varepsilon_{\mathrm{max}}$] ($M^{-1}$ cm^{-1}): 661 [35], 301 [580], 255 [7170]. Selected IR bands (KBr disk), υ(cm^{-1}): 3549 s, 3445 s, 3356 s, 3067 s br, 1650 s, 1615 s, 1487 w, 1450 m, 1314 w, 1292 w, 1254 w, 1054 s br, 929 w, 868 w, 820 w, 768 m, 726 w. Crystals suitable for X-ray crystallography were grown by diffusing diethyl ether into a methanolic solution of the complex and were of composition $[Cu(L^1H^+)(MeOH)](ClO_4)_3\cdot MeOH$.

$[Cu(L^2H^+)(OH_2)](ClO_4)_3\cdot 2NaClO_4\cdot 4H_2O$ (C2) and $[Cu(L^2H^+)(OH_2)](ClO_4)_3\cdot H_2O$ (C2′). This complex was isolated as dark blue crystals following the same procedure described for **C1**, starting from $Cu(NO_3)_2\cdot 3H_2O$ (0.483 g, 2.16 mmol) and L^2·HCl (0.386 g, 1.15 mmol). Yield: 0.314 g, 27.3%. Anal. calcd for $C_{16}H_{33}Cl_5CuN_6O_{25}Na_2$: C, 19.3; H, 3.3; N, 8.4%. Found: C, 19.2; H, 3.1; N, 8.3%. UV−vis (H_2O), λ_{max} (nm) [$\varepsilon_{\mathrm{max}}$] ($M^{-1}$ cm^{-1}): 660 [65], 255 [6810]. Selected IR bands (KBr disk), υ(cm^{-1}): 3451 s, 3370 s, 3232 s, 2954 m, 2051 w, 1662 s, 1615 s, 1483 w, 1450 m, 1388 w, 1317 w, 1292 w, 1034 s br, 930 m, 770 m. Crystals suitable for X-ray crystallography were grown by slow evaporation of an aqueous solution of the complex and were of composition $[Cu(L^2H^+)(OH_2)](ClO_4)_3\cdot H_2O$.

$[Cu(L^3H^+)(OH_2)](ClO_4)_3\cdot NaClO_4$ (C3) and $[Cu(L^2H^+)(OH_2)](ClO_4)_3\cdot H_2O$ (C3′). This complex was isolated as dark blue crystals following the same procedure described for **C1**, starting from $Cu(NO_3)_2\cdot 3H_2O$ (0.506 g, 2.26 mmol) and L^3·HCl (0.319 g, 0.914 mol). Yield: 0.255 g, 34.2%. Anal. calcd for $C_{17}H_{27}Cl_4CuN_6O_{17}Na$: C, 25.0; H, 3.3; N, 10.3%. Found: C, 25.1; H, 3.5; N, 10.2%. UV−vis (H_2O), λ_{max} (nm) [$\varepsilon_{\mathrm{max}}$] ($M^{-1}$ cm^{-1}): 649 [30], 255 [5100]. Selected IR bands (KBr disk), υ(cm^{-1}): 3552 m, 3376 s, 3312 s, 3233 s, 3068 m, 2975 m, 2052 w, 1661 s, 1616 s, 1576 w, 1475 w, 1451 m, 1382 w, 1318 w, 1286 w, 1260 w, 1161 m, 1083 s br, 1031 s br, 923 m, 861 m, 776 m. Crystals suitable for X-ray crystallography were grown as in the case of **C2′** and were of composition $[Cu(L^3H^+)(OH_2)](ClO_4)_3\cdot H_2O$.

DNA Cleavage Experiments. Reaction mixtures (total volume 15 μL), containing pBR 322 supercoiled plasmid DNA (38 μM base-pair, bp, concentration) and a copper complex (150 μM) dissolved in HEPES buffer (40 mM, pH 7.2), were incubated at 37 °C for up to 48 h. A loading buffer (0.1 M EDTA, 40% (w/v) sucrose, 0.05% (w/v) bromophenol blue, and 0.5% (w/v) sodium lauryl sulfate; 5 μL) was added to end the reactions at defined time periods, and the resulting mixtures were stored at −20 °C until just prior to analysis. Mixtures were then loaded onto 1% agarose gels containing 1.0 μg dm^{-3} EB, and the DNA fragments were separated by gel electrophoresis (70 V for 2 h in 1 × Tris-acetate EDTA (TAE) buffer). Ethidium-stained agarose gels were imaged, and the extent of supercoiled DNA cleavage was determined *via* densitometric analysis of the visualized bands using the volume quantitation method. In all cases, background fluorescence was determined by reference to a lane containing no DNA. Supercoiled pBR 322 DNA values were corrected by a factor of 1.42 to account for the greater ability of ethidium bromide to intercalate into supercoiled DNA (form I) compared to nicked DNA (form II).[41] The relative amounts of the different forms of DNA were determined by dividing the fluorescence intensity of each band by

the sum of fluorescence intensities for all bands in that lane. All experiments were performed at least in duplicate.

Phosphate Ester Cleavage Kinetics. *bis*(*p*-Nitrophenyl)-phosphate (BNPP). These experiments were conducted as previously described.[12,13] Briefly, the rate of cleavage of BNPP by the Cu(II) complexes was measured at pH 7.4 (MOPS buffer) or 9 (CHES buffer), $T = 50$ °C, by following the formation of *p*-nitrophenoxide (NP) ion ($\lambda_{max} = 400$ nm, $\varepsilon_{max} = 18\,700\ M^{-1}cm^{-1}$) in solutions containing 15 μM BNPP and a 1 mM Cu(II) complex and $I = 0.15$ M ($NaClO_4$), on a Varian Cary 3 spectrophotometer. Absorbance measurements were commenced 2 min after mixing and were continued for 8000 min, with a reading taken every 5 min. As the complex was in large excess compared to BNPP, the appearance of NP (and cleavage of BNPP) was modeled as a first-order process, $Abs = A + Be^{-k_{obs}t}$, or using the initial rates method described previously.[9]

Uridine-3′-*p*-nitrophenylphosphate (UpNP). These experiments were carried out in a similar manner to the BNPP experiments. Briefly, a solution (total volume 2.5 mL) containing the Cu(II) complex (200 μM), a MOPS or CHES buffer (50 mM, pH 6.5 or 7.4 (9.0 for CHES) at the appropriate temperature (25 or 37 °C)), and $NaClO_4$ (final ionic strength = 150 mM) was placed in a quartz cuvette cell and allowed to equilibrate at the desired experimental temperature for 15 min. After this time, 10 μL of UpNP (5 mM) was added (final [UpNP] = 20 μM), and data collection was begun immediately. Absorbance measurements were made at 400 nm for 1 h, recording data every 3 s. The data were again fitted to the equation $Abs = A + Be^{-k_{obs}t}$, which models the observed substrate cleavage (release of NP) as a first-order process.

Solution Speciation Studies. A series of solutions (total volume 600 μL) were prepared containing MOPS (50 mM, solution pH = 6.0, 6.5, 7.0, 7.5, 7.75, and 8.0 at 25 °C), $NaClO_4$ (100 mM), and one of the Cu(II) complexes ([**C1**] = 3.99 mM, [**C2**] = 4.95 mM, [**C3**] = 7.05 mM). Each solution was then equilibrated at 25 °C for 15 min, at which point the UV−vis−NIR spectrum was measured. Each spectrum was background-corrected using the MOPS buffer as the blank. In the case of **C1**, deprotonation and coordination of the guanidine pendant arm occurred according to

$$[Cu(LH)(OH_2)_3]^{3+} \overset{K_{app}}{\rightleftharpoons} [Cu(L)(OH_2)_2]^{2+} + H_3O^+ \quad (1)$$

In the case of $[Cu(DPA)(OH_2)_2]^{2+}$, **C2** and **C3** deprotonation of a coordinated water molecule occurs according to

$$[Cu(LH)(OH_2)_3]^{3+} \overset{K_a}{\rightleftharpoons} [Cu(LH)(OH_2)_2]^{2+} + H^+ \quad (2)$$

Although these two processes are different, the mathematical expressions used to fit the pH dependence of the absorbance are identical. The Igor Pro software package was used to determine values of k_{app} and k_a by analyzing the change in absorbance with pH at selected wavelengths of maximum change.

X-Ray Crystallography. Intensity data for blue crystals of **C1′** (0.31 × 0.21 × 0.10 mm), **C2′** (0.15 × 0.15 × 0.05 mm), and **C3′** (0.15 × 0.10 × 0.09 mm) were collected at 123 K on a Bruker Apex II CCD fitted with graphite monochromated Mo Kα radiation (0.71073 Å). The data were collected to a maximum 2θ value of 55° (60° for **C1′**) and processed using the Bruker Apex II software package. Crystal parameters and details of the data collection are summarized in Table 1.

Scheme 1. Synthesis of Hydrochloride Salts of L^1, L^2, and L^3

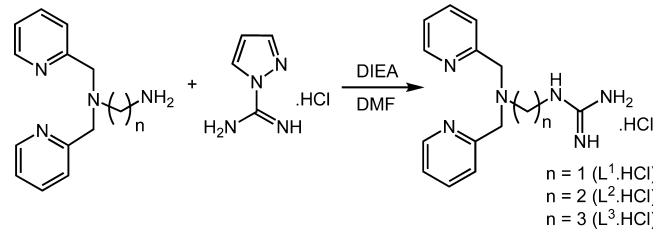

C2′ was a medrohedral twin, and the cell was indexed using CELL_NOW[42] and scaled with TWINABS, which wrote the HKLF4/5 file.[43] The structure was then solved (using the major twin component) by direct methods using the SHELX-97[44,45] software package and refined against the HKLF5 file. The structures of **C1′** and **C3′** were solved using SHELX-97 and expanded using standard Fourier transform routines. All hydrogen atoms were placed in idealized positions, except that for the alcoholic and water hydrogens, which were located on the Fourier difference maps (H2M in **C1′** was located as a Fourier difference peak, and its position was not refined). Two of the noncoordinating perchlorate anions in **C1′** were severely disordered and had the site occupancy of their components refined against each other. All non-hydrogen atoms were refined anisotropically.

Results and Discussion

Preparation of Ligands and Copper(II) Complexes. The three new DPA ligand derivatives, bearing guanidinium pendants of varying lengths, were prepared in high yield (88−94%) by reacting the corresponding *N*,*N*-*bis*(2-pyridylmethyl)alkane-α,*ω*-diamines with 1*H*-pyrazole-1-carboxamidine hydrochloride in DMF (Scheme 1). Separation of the products from the reaction mixtures (as hydrochloride salts) was readily achieved through the addition of diethyl ether and cooling to 4 °C. The resulting oils that separated out were found to be spectroscopically pure. Electrospray mass spectra showed *m*/*z* peaks at 285.2, 299.2, and 313.2, corresponding to the molecular ions, $[M + H]^+$, of the ligands L^1, L^2, and L^3, respectively.

The copper(II) complexes of the ligands were prepared by reacting the hydrochloride salts of the ligands with $Cu(NO_3)\cdot 3H_2O$ in aqueous solution, to produce dark-blue-colored solutions. Following cation exchange chromatography, using aqueous $NaClO_4$ as the eluent, the complexes crystallized in the form of long blue needles. Elemental analyses revealed the composition of these to be $[Cu(LH^+)(OH_2)](ClO_4)_3\cdot x NaClO_4\cdot y H_2O$ (**C1**: L = L^1, $x = 2$, $y = 3$; **C2**: L = L^2, $x = 2$, $y = 4$; **C3**: L = L^3, $x = 1$, $y = 0$). Vapor diffusion of diethyl ether into a methanolic solution of **C1** and recrystallization of **C2** and **C3** from aqueous solutions yielded crystals of $[Cu(L^1H^+)(MeOH)](ClO_4)_3\cdot MeOH$ (**C1′**) and $[Cu(LH^+)(OH_2)](ClO_4)_3\cdot H_2O$ (**C2′**: L = L^2; **C3′**: L = L^3), all of which were suitable for X-ray crystallography.

(41) An, Y.; Tong, M. J.; Ji, L.-N.; Mao, Z.-W. *J. Chem. Soc., Dalton Trans.* **2006**, 2066–2071.
(42) Sheldrick, G. M. *CELL_NOW*; Bruker-AXS, Inc.: Madison, WI, 2004.
(43) Sheldrick, G. M. *TWINABS*; University of Göttingen: Göttingen, Germany, 2002.
(44) Sheldrick, G. M. *SHELXL-97*; University of Göttingen: Göttingen, Germany, 1997.
(45) Sheldrick, G. M. *SHELXS-97*; University of Göttingen: Göttingen, Germany, 1997.

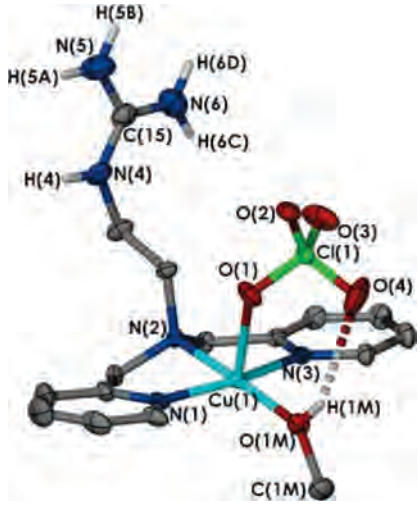

Figure 3. Thermal ellipsoid plot of the complex cation unit in **C1′** with counterions, noncoordinating methanol molecule and selected hydrogen atoms removed for clarity (ellipsoids drawn at 50% probability level).

Table 2. Selected Bond Lengths [Å] and Angles [deg] for **C1′**[a]

Cu(1)−N(3)	1.955(2)	N(3)−Cu(1)−N(1)	166.58(9)
Cu(1)−N(1)	1.956(2)	N(3)−Cu(1)−N(2)	83.58(8)
Cu(1)−O(1M)	1.997(2)	N(1)−Cu(1)−N(2)	83.50(9)
Cu(1)−N(2)	2.032(2)	O(1M)-Cu(1)−N(2)	178.08(9)
Cu(1)−O(1)	2.438(2)	N(3)−Cu(1)−O(1)	101.25(7)
Cu(1)−O(2)#1	2.629(2)	N(1)−Cu(1)−O(1)	84.62(8)
		O(1M)−Cu(1)−O(1)	81.73(8)
		N(2)−Cu(1)−O(1)	100.11(8)
		N(3)−Cu(1)−O(1M)	96.62(8)
		N(1)−Cu(1)−O(1M)	96.17(9)

[a] Symmetry transformations used to generate equivalent atoms: #1 x, $y - 1$, z.

Table 3. Hydrogen-Bonding Interactions in **C1′** [Å and deg][a]

D−H···A	d(D−H)	d(H···A)	d(D···A)	<(DHA)
O(1M)−H(1M)···O(4)	0.75(5)	2.45(5)	3.112(4)	148(5)
O(2M)−H(2M)···O(10A)#1	0.802(3)	1.980(6)	2.771(6)	169.0(3)
N(4)−H(4)···O(7B)	0.88	2.1	2.968(7)	170
N(4)−H(4)···O(7A)	0.88	2.32	3.054(7)	141
N(4)−H(4)···O(8B)#2	0.88	2.47	2.91(1)	111
N(5)−H(5B)···O(9)#3	0.88	2.14	2.999(5)	167
N(5)−H(5A)···O(7A)#4	0.88	2.19	2.984(7)	150
N(5)−H(5A)···O(8A)	0.88	2.58	3.30(1)	140
N(6)−H(6C)···O(2M)	0.88	1.94	2.724(5)	148
N(6)−H(6C)···O(10B)#1	0.88	2.51	3.31(1)	153
N(6)−H(6D)···O(12A)#3	0.88	2.09	2.919(4)	157

[a] Symmetry transformations used to generate equivalent atoms: #1 $x - 1/2$, $-y + 1/2$, $z - 1/2$; #2 $-x + 1/2$, $y - 1/2$, $-z + 1/2$; #3 $x - 1/2$, $-y + 3/2$; $z - 1/2$, #4 $-x + 1/2$, $y + 1/2$, $-z + 1/2$.

X-Ray Crystal Structures. The X-ray structure determination of **C1′** reveals a mononuclear, *pseudo*-square pyramidal/octahedral copper(II) complex (Figure 3). Three of the basal coordination sites are occupied by the nitrogens of the DPA ligand, with the Cu−N distances associated with the two pyridyl N donors (1.95 Å) being slightly shorter than that for the tertiary amine donor (2.032(2) Å; see Table 2 for selected bond angles and distances and Table 3 for hydrogen-bonding interactions). The other donor in the basal plane is an oxygen from a methanol molecule, Cu−O distance of 1.997(2) Å, while one apical position is occupied by a weakly coordinating perchlorate, Cu−O distance of 2.438(2) Å. This perchlorate anion is involved in hydrogen-bonding to the hydroxyl proton of the coordinated methanol molecule.

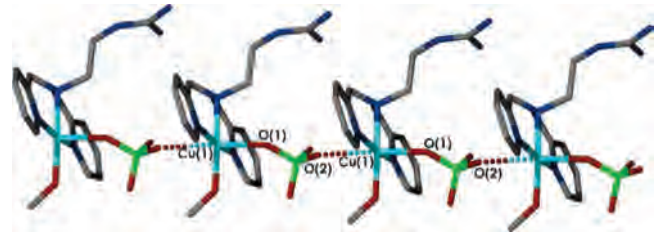

Figure 4. Stick representation of **C1′** highlighting the linear chain of complex cation units formed as a result of the *pseudo*-bridging binding mode of the coordinated perchlorate anions (dashed bonds indicate weak bonding interaction).

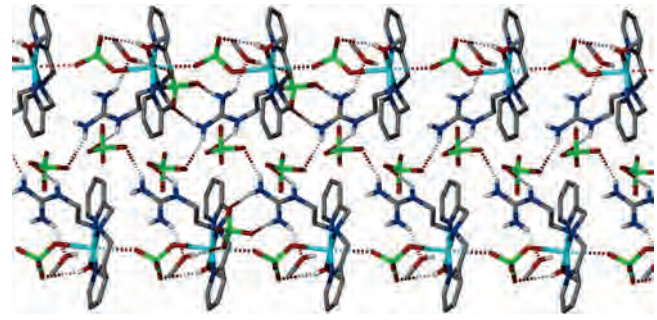

Figure 5. Stick diagram showing the extensive hydrogen bonding within the crystal lattice of **C1′** (dashed lines indicate hydrogen bonds).

Within the equatorial plane, the complex exhibits distortion typical for DPA-type complexes, with all of the N−Cu−N angles lying below 90° as a result of the constraints imposed by the tridentate DPA moiety. This distortion is reflected in a τ value of 20%. This parameter is often used to estimate the degree of distortion from ideal square-pyramidal geometry ($\tau = 0\%$) toward trigonal bipyramidal geometry ($\tau = 100\%$) in five-coordinate complexes.[46]

In addition to the above contacts, the Cu(II) center forms a weak interaction with an oxygen (Cu−O = 2.629(2) Å) from a perchlorate ion that is bound to the Cu(II) center of an adjacent complex unit. As a consequence, the complex cation units within the crystal lattice are arranged in infinite linear chains (Figure 4). Axially coordinating perchorates have been observed in other DPA complexes. For example, in the X-ray structure of the copper(II) complex of *bis*(6-methyl-2-pyridylmethyl)amine, isolated by Yamaguchi and co-workers,[47] two perchlorate anions coordinate at either pole of a distorted octahedral Cu(II) coordination sphere, with Cu−O distances of 2.441(2) and 2.810(2)Å, the latter being significantly weaker than in **C1′**.

The guanidinium pendant of L^1 projects away from the Cu(II) center and is involved in charge-assisted hydrogen-bonding interactions with two noncoordinated perchlorate anions and a cocrystallized methanol molecule (Figure 5). This results in a two-dimensional hydrogen-bonding network within the crystal lattice that is two complex cation units wide and one cation unit deep. The propensity of guani-

(46) Addison, A. W.; Rao, T. N.; Reedijk, J.; Van Rijn, J.; Verschoor, G. C. *Dalton Trans.* **1984**, 49–1356.
(47) Yokoyama, H.; Yamaguchi, K.; Sugimoto, M.; Suzuki, S. *Eur. J. Inorg. Chem.* **2005**, *2005*, 1435–441.

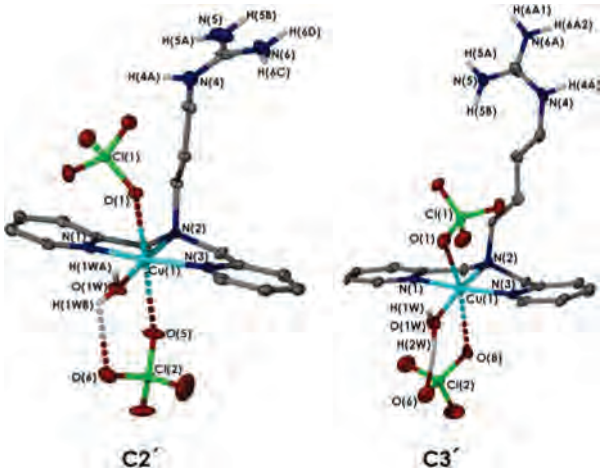

Figure 6. Thermal ellipsoid plots of **C2′** and **C3′** with a counterion, solvent water, and selected hydrogen atoms removed for clarity (ellipsoids are drawn at the 50% probability level; dashed bonds indicate hydrogen- and weak-bonding interactions).

Table 4. Selected Bond Lengths [Å] and Angles [deg] for **C2′** and **C3′**

		C2′	
Cu(1)−N(3)	1.977(3)	N(3)−Cu(1)−N(1)	166.24(1)
Cu(1)−N(1)	1.981(3)	N(3)−Cu(1)−O(1W)	95.56(1)
Cu(1)-O(1W)	1.984(3)	N(1)−Cu(1)−O(1W)	97.91(1)
Cu(1)−N(2)	2.032(3)	N(3)−Cu(1)−N(2)	82.95(1)
Cu(1)−O(1)	2.489(3)	N(1)−Cu(1)−N(2)	83.44(1)
Cu(1)−O(5)	2.454(3)	O(1W)-Cu(1)−N(2)	176.32(1)
		C3′	
Cu(1)−N(3)	1.975(4)	N(3)−Cu(1)−N(1)	166.84(2)
Cu(1)−N(1)	1.978(4)	N(3)−Cu(1)−O(1W)	98.23(2)
Cu(1)-O(1W)	1.993(4)	N(1)−Cu(1)−O(1W)	94.05(2)
Cu(1)−N(2)	2.035(4)	N(3)−Cu(1)−N(2)	83.57(2)
Cu(1)−O(1)	2.386(4)	N(1)−Cu(1)−N(2)	83.45(2)
Cu(1)−O(8)	2.625(4)	O(1W)−Cu(1)−N(2)	168.45(2)

dinium groups to form multiple hydrogen bonds is well-established.[48]

The crystal structures of **C2′** and **C3′** are broadly similar to each other and share several common features with the structure of **C1′** (see Figure 6). Upon first inspection, the copper(II) center may be considered to reside in a square-planar coordination environment, bound by the three nitrogen atoms of the DPA moiety and a water molecule. The Cu−O and Cu−N distances (Table 4) are very similar to those found for **C1′**. However, two perchlorate anions form weak axial interactions with each copper(II) center, so the complexes can also be considered to possess *pseudo*-octahedral geometry. The coordination polyhedron of **C2′**, with Cu−O(perchlorate) distances of 2.489(3) and 2.454(3) Å, is somewhat more symmetrical than that of **C3′**, which has disparate Cu−O(perchlorate) distances of 2.386(4) and 2.625(4) Å.

A feature common to the structures of both **C2′** and **C3′** is the presence of an *intra*molecular hydrogen bond between the coordinated water and one of the coordinated perchlorate ions, similar to that found for the coordinated methanol in **C1′**. This is the only *intra*molecular hydrogen bond within the structures. However, an extended *inter*molecular hydrogen-bonding network is centered around the guanidinium hydrogen-bond donors, with the perchlorate anion oxygens acting as acceptors (see Figures 7 and 8 and Tables 5 and 6). In the case of **C2′**, the network extends in all three dimensions, with each guanidinium group forming hydrogen bonds with four different perchlorate molecules, each of which acting as a hydrogen-bond acceptor to two adjacent complex cations. There is also a cocrystallized water molecule, which hydrogen-bonds to a coordinated water on one complex

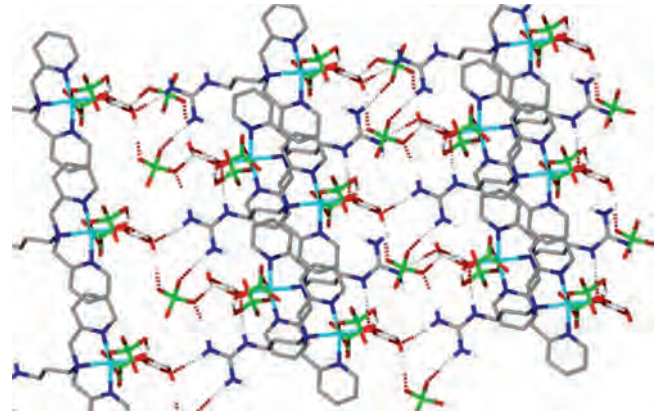

Figure 7. Stick diagram showing the extensive hydrogen bonding within the crystal lattice of **C2′** (dashed lines indicate hydrogen bonds).

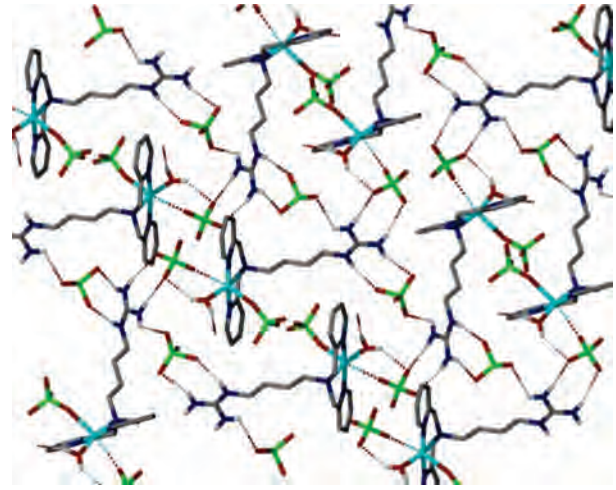

Figure 8. Stick diagram showing the extensive hydrogen bonding within the crystal lattice of **C3′** (dashed lines indicate hydrogen bonds; hydrogen-bonding interactions involving the cocrystallized water are not shown as the water hydrogens were not able to be located).

Table 5. Hydrogen-Bonding Interactions in **C2′** [Å and deg][a]

D−H···A	*d*(D−H)	*d*(H···A)	*d*(D···A)	<(DHA)
N(4)−H(4A)···O(4)#1	0.88	2.15	3.020(5)	168
N(5)−H(5A)···O(11)#2	0.88	2.18	3.042(7)	166
N(5)−H(5B)···O(2W)#3	0.88	2.08	2.931(5)	163
N(6)−H(6C)···O(3)#4	0.88	2.43	3.233(5)	151
N(6)−H(6D)···O(9)#5	0.88	2.17	2.976(6)	152
O(2W)−H(2WA)···O(4)	0.81(5)	2.24(5)	2.942(5)	147(4)
O(2W)−H(2WA)···O(11)#6	0.81(5)	2.42(5)	3.054(6)	136(4)
O(1W)−H(1WB)···O(10)#7	0.71(6)	2.35(6)	3.036(6)	166(7)
O(1W)−H(1WB)···O(6)	0.71(6)	2.44(6)	2.841(4)	118(6)
O(2W)−H(2WB)···O(12)#8	0.71(9)	2.21(9)	2.907(6)	168(11)
O(1W)−H(1WA)···O(2W)	0.84(7)	1.89(7)	2.701(4)	164(6)

[a] Symmetry transformations used to generate equivalent atoms: #1 $-x+1, -y+1, -z$; #2 $-x+3/2, y+1/2, -z+1/2$; #3 $x, y+1, z$; #4 $-x, -y+1, -z$; #5 $-x+1/2, y+1/2, -z+1/2$; #6 $x-1/2, -y+1/2, z-1/2$; #7 $-x+3/2, y-1/2, -z+1/2$; #8 $-x+1/2, y-1/2, -z+1/2$.

(48) Hubberstey, P.; Suksangpanya, U. *Struct. Bonding (Berlin)* **2004**, *111*, 33–83.

Table 6. Hydrogen-Bonding Interactions in **C3′** [Å and deg][a]

D−H···A	*d*(D−H)	*d*(H···A)	*d*(D···A)	<(DHA)
O(1W)−H(1W)···O(2W)	0.977(5)	1.711(5)	2.671(7)	166.6(3)
O(1W)−H(2W)···O(6)	0.85(7)	2.24(8)	2.969(7)	144(6)
O(1W)−H(2W)···O(10)#1	0.85(7)	2.62(7)	3.150(7)	121(6)
N(4)−H(4A)···O(12A)#2	0.88	2.54	3.338(15)	151
N(5)−H(5A)···O(6)#3	0.88	2.2	3.078(6)	174
N(5)−H(5B)···O(9)	0.88	2.62	3.199(10)	124
N(6A)−H(6A1)···O(7)#3	0.88	2.42	3.279(10)	165
N(6A)−H(6A2)···O(12A)#2	0.88	2.3	3.149(15)	161

[a] Symmetry transformations used to generate equivalent atoms: #1 $x-1, -y+1/2, z-1/2$; #2 $-x+1, y+1/2, -z+3/2$; #3 $x+1, -y+1/2, z+1/2$.

cation and the guanidine pendant of an adjacent cation unit. The hydrogen-bonding network in **C3′** is nearly identical to that found in **C2′**; however, the hydrogen atoms on the cocrystallized water were not able to be located on the Fourier difference map, so that the full extent of the hydrogen-bonding network could not be established. The only other subtle differences are as follows: (i) the guanidinium group in **C3′** hydrogen-bonds to three, rather than four, perchlorate anions, and (ii) adjacent guanidinium groups in **C3′** are skewed relative to one another (angle of 69.27(3)° between their least-squares planes), whereas in **C2′**, the planes of the guanidinium groups all lay parallel to one another.

Solution Speciation Studies. To better understand the solution behavior of complexes **C1**−**C3**, a series of pH titrations were performed which monitored changes in the UV−vis−NIR spectrum of the complexes as a function of the pH (see Figure 9). It is immediately evident from the data in Figure 9 that a major pH-dependent spectral change is observed only for **C1**. As pH increases, distinct bands are observed above 800 nm, which are indicative of d → d transitions. The appearance of these bands is consistent with a change in the geometry of the copper(II) center from a distorted octahedral at low pH to square-pyramidal at higher pH, achieved through binding of the deprotonated guanidine pendant arm at higher pH (see Figure 10).[49] This guanidine binding mode has been previously documented in work by Kimura *et al.*[50] with a Zn(II)-cyclen compound which also has two methylene units linking the guanidium group to the macrocycle.

Analysis of the systematic increase in intensity of these bands at increasing pH allowed the determination of an apparent acidity constant, "pK_{app}", for the deprotonation and coordination of the guanidine group. Interestingly, the pK_{app} value of 6.95 ± 0.09 is some 5−6 pH units lower than the pK_a value for the guanidinium ion and for deprotonation of the guanidinium group in argininine. This demonstrates that there is a strong driving force for the formation of a seven-membered chelate ring involving the guanidine pendant.

Compounds **C2** and **C3** did not show any major change in spectral behavior that could be ascribed to a significant change in copper(II) geometry or coordination sphere occupancy. For these complexes, the formation of eight- and nine-membered chelate rings involving the deprotonated guanidine pendant is obviously not favored energetically, and the complexes retain their original geometry. Small but systematic changes in absorption were observed at 340 nm for both **C2** and **C3**. Analysis of this change in absorbance with pH allowed the pK_a of water coordinated to these complexes to be estimated (see Table 7). **C3** has a pK_a similar to that previously measured for the parent Cu(II)−DPA compound, whereas that for **C2** is substantially lower. This could potentially be due to the closer proximity of the charged guanidine pendant in **C2**, inductively lowering the pK_a of the coordinated water. Notably, the pK_a of the copper(II) complex of an *N*-amide-functionalized DPA

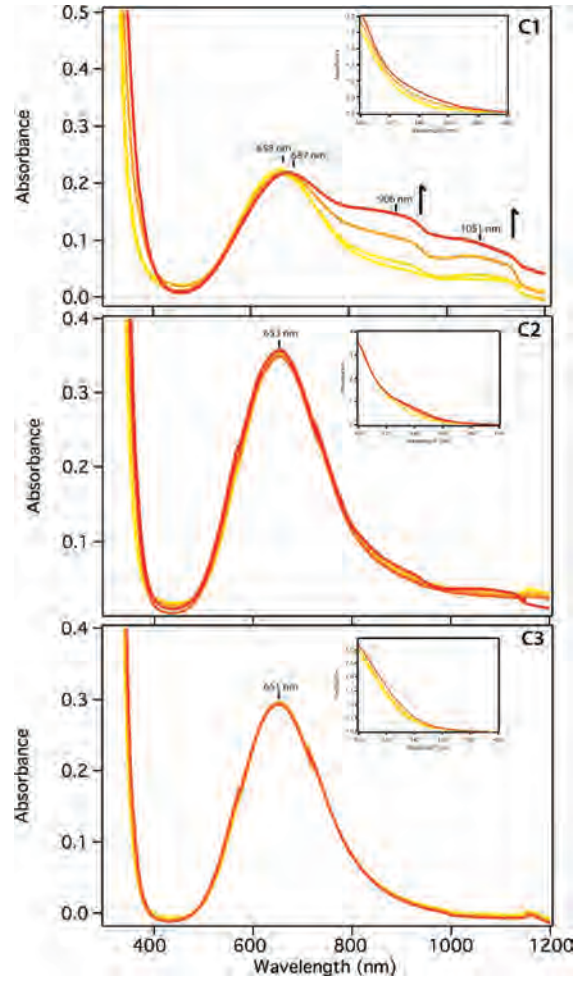

Figure 9. UV−vis−NIR spectra of complexes **C1**−**C3** at variable pH. Yellow traces, pH = 6.0; red traces, pH = 8.0. Conditions: [**C1**] = 3.99 mM, [**C2**] = 4.95 mM, [**C3**] = 7.05 mM, [MOPS] = 50 mM (pH = 6.0, 6.5, 7.0, 7.5, 8.0 at 25 °C), [$NaClO_4$] = 100 mM.

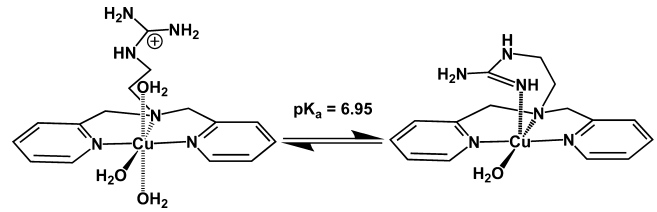

Figure 10. Proposed solution structures for **C1** with the guanidine pendant arm cyclizing onto the Cu(II) center.

(49) Cotton, F. A. *Advanced Inorganic Chemistry*, 6th ed.; John Wiley & Sons: New York, 1999.
(50) Aoki, S.; Iwaida, K.; Hanamoto, N.; Shiro, M.; Kimura, E. *J. Am. Chem. Soc.* **2002**, *124*, 5256–5257.

Table 7. pK_a values calculated from the increase in absorbance intensity at 340 nm

compound	pK_a (coordinatedH_2O)	ref
$[Cu(DPA)(OH_2)_3]^{2+a}$	8.6	52
$[Cu(DPA)(OH_2)_3]^{2+}$	8.14 ± 0.14	this work
C1	not observed	this work
C2	7.02 ± 0.14	this work
C3	8.79 ± 0.04	this work
$[Cu(OPDPA)(OH_2)_3]^{2+a}$	7.8	51

[a] Complex solution was prepared by dissolving $[Cu(DPA)Cl_2]$ in water measured by potentiometric titration. OPDPA = *N*-(3-octadecylpropanamido)*bis*(2-pyridylmethyl)amine.

Table 8. First-Order Rate Constants for Hydrolysis of BNPP by Copper(II) Complexes (Standard Error in Parentheses)[a]

compound	k_{obs} ($\times 10^7$ s^{-1}) pH = 7.4	pH = 9.0
$[Cu(DPA)(OH_2)_3]^{2+}$ [b]	44.2(6)	115.4(2)
C1	3.05(4)	0.145(6)
C2	2.10(7)	4.96(9)
C3	4.41(8)	3.33(3)

[a] Conditions used: [complex] = 0.1 mM, [BNPP] = 0.015 mM, I = 0.15 M, T = 50 °C, buffered with MOPS (pH 7.4) or CHES (pH 9). [b] Complex solution was prepared by dissolving $[Cu(DPA)Cl_2]$ in water.

derivative was found to be on the order of 7.8,[51] indicating that the appended functional group significantly attenuates the acidity.

Cleavage of Model Phosphate Esters. To probe the phosphate ester cleavage properties of **C1**−**C3**, their reactivity toward the well-known activated phosphodiester, BNPP, was investigated. BNPP has been extensively employed in cleavage studies due the fact that one hydrolytic product, *p*-nitrophenoxide anion, is highly colored (λ_{max} = 400 nm), allowing the cleavage of BNPP to be monitored by spectrophotometry (see Experimental Section).

Interestingly, in contrast to the DNA cleavage results (*vide infra*), complexes **C1**−**C3** were found to be significantly less active in cleaving BNPP than the parent DPA complex, $[Cu(DPA)(OH_2)_3]^{2+}$. The first-order rate constants for BNPP cleavage by **C1**−**C3** at pH 7.4 (Table 8) were found to be an order of magnitude lower than that for $[Cu(DPA)(OH_2)_3]^{2+}$, and much less reactive than other copper(II) complexes of tridentate ligands reported by us in the literature.[12,53] When tested at a higher pH of 9.0, the rate of cleavage of BNPP by **C1** was found to decrease dramatically (20-fold), while that for **C2** and **C3** remained largely unaffected. The rate of cleavage by the parent DPA complex more than doubled. At this stage, the exact reasons for the lower overall reactivity of all three complexes of the ligands with guanidinium pendants are unclear. The guanidinium groups in these complexes could become involved in interactions (e.g., H-bonding) with this particular model phosphate ester, which render it less reactive than when bound to the parent DPA complex. For **C1**, the even slower rate of BNPP hydrolysis at pH 9 can be attributed to the coordination of the guanidine pendant, as reported by Kimura *et al.*,[50] which makes the resulting complex substantially less active.

Scheme 2. Cyclization of UpNP by Attack of the 2′-OH Internal Nucleophile

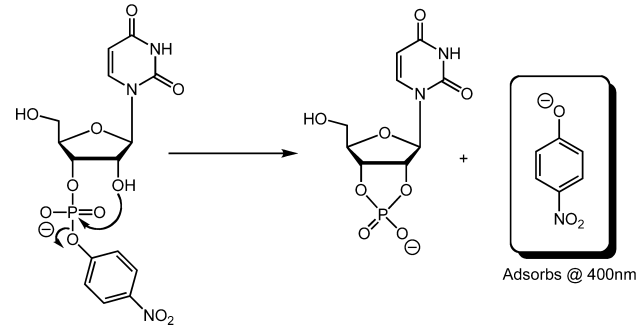

Table 9. First-Order Observed Rates of the Transesterification of UpNP by Copper(II) Complexes (Standard Error in Parentheses)[a]

	pH = 6.5 k_{obs} ($\times 10^4$ s^{-1})	pH = 7.4 k_{obs} ($\times 10^4$ s^{-1})	pH = 9.0 k_{obs} ($\times 10^2$ s^{-1})
	T = 25 °C		
background cyclization	1.4(2)	18.0(4)	4.6(1)
$[Cu(tacn)(OH_2)_2]^{2+}$	2.41(4)	25(2)	5.0(3)
$[Cu(Me_3tacn)(OH_2)_2]^{2+}$	1.8(2)	19(1)	5.1(2)
$[Cu(DPA)(OH_2)_3]^{2+}$	3.2(1)	36(2)	5.8(5)
C1	7.4(2)	33(3)	4.70(9)
C2	3.19(9)	26(2)	12.4(8)
C3	3.3(1)	48(3)	12.3(2)
	T = 37 °C		
background cyclization	3.33(9)	44(3)	N/M
$[Cu(tacn)(OH_2)_2]^{2+}$	6.4(2)	62(4)	N/M
$[Cu(Me_3tacn)(OH_2)_2]^{2+}$	4.53(2)	50(3)	N/M
$[Cu(DPA)(OH_2)_3]^{2+}$	7.4(4)	88(7)	N/M
C1	18.5(7)	72(3)	N/M
C2	8.5(2)	100(5)	N/M
C3	8.54(6)	109(4)	N/M

[a] Conditions used: [complex] = 200 μM, [UpNP] = 20 μM, I = 0.15 M, buffered with MOPS (pH 7.4 or 6.5) or CHES (pH 9). Me_3tacn = 1,4,7-trimethyl-1,4,7-triazacyclononane, tacn = 1,4,7-triazacyclononane. N/M: rate too fast to measure by conventional spectrophotometric methods.

As a further extension of this work, the cleavage of an RNA mimic, UpNP, by the copper(II) complexes was also investigated. As in the case of RNA, this compound can undergo cleavage *via* an *intra*molecular transesterification reaction, involving nucleophilic attack of the 2′-OH of the ribose sugar on the 3′-linked phosphate group (Scheme 2). This cyclization reaction is easily monitored again by following the release of the *p*-nitrophenoxide chromophore.

The measured rates of UpNP cleavage by the copper(II) complexes at two different temperatures and pH values are summarized in Table 9. For comparison purposes, the rate of cleavage of UpNP by the copper(II) complexes of 1,4,7-triazacyclononane (tacn) and 1,4,7-trimethyl-1,4,7-triazacyclononane (Me_3tacn) was also determined, since we and others have previously shown these to be effective phosphate ester cleavage agents.[3,4,8−10] It is clear that, while the DPA complexes are not as active in hydrolyzing BNPP as, for example, $[Cu(Me_3tacn)(OH_2)_2]^{2+}$,[10] they are more effective in cleaving the RNA mimic. Under the conditions tested, the parent DPA complex, $[Cu(DPA)(OH_2)_3]^{2+}$, was itself found to cleave UpNP approximately 2 times faster than the background rate, compared to the tacn-based complexes,

(51) Bhattacharya, S.; Snehalatha, K.; Kumar, V. P. *J. Org. Chem.* **2003**, *68*, 2741–2747.
(52) Nakon, R.; Rechani, P. R.; Angelici, R. J. *J. Am. Chem. Soc.* **1974**, *96*, 2117–2120.
(53) Belousoff, M. J.; Battle, A. R.; Graham, B.; Spiccia, L. *Polyhedron* **2007**, *26*, 344–355.

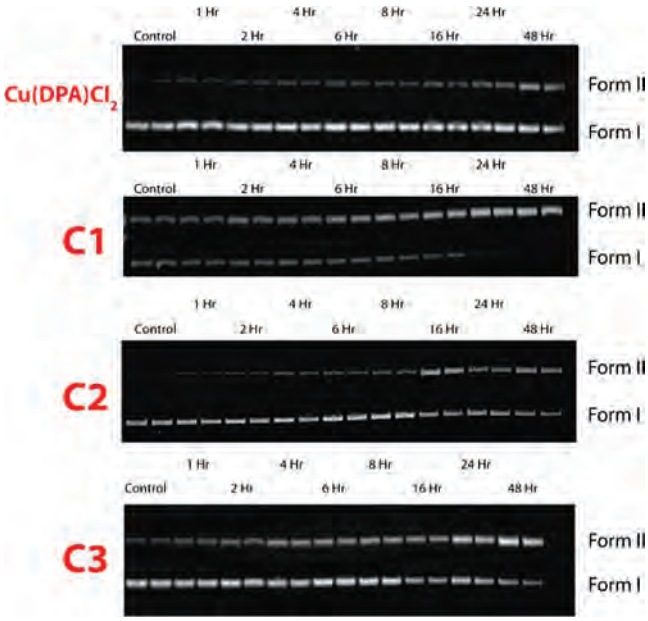

Figure 11. Agarose gel showing the cleavage of pBR 322 plasmid DNA (38 μM bp) incubated with Cu(DPA)Cl_2 and **C1**−**C3** (150 μM) in HEPES buffer (40 mM, pH 7.2) at 37 °C for various time intervals. Lanes 1 and 2: DNA control. Lanes 3 and 4: 1 h. Lanes 5 and 6: 2 h. Lanes 7 and 8: 4 h. Lanes 9 and 10: 6 h. Lanes 11 and 12: 8 h. Lanes 13 and 14: 16 h. Lanes 15 and 16: 24 h. Lanes 17 and 18: 48 h.

Table 10. Observed Rate Constant k_{obs} for Single-Strand Cleavage of pBR 322 Plasmid DNA by Copper(II) Complexes (Standard Error in Parentheses) Determined at pH =7.2[a]

compound	k_{obs} ($\times$ 10^6 s^{-1})
$[Cu(DPA)(OH_2)_3]^{2+}$	1.0(1)
C1	9(2)
C2	10(3)
C3	7(3)

[a] Conditions used: [complex] = 150 μM, [pBR 322 plamid] = 38 μM (per bp), [HEPES] = 40 mM (pH = 7.2 at 37 °C). Data were analyzed using first-order analysis, yielding k_{obs} directly.

which barely enhanced cleavage above background levels. Complexes **C1**−**C3** were generally found to be as reactive, and in some cases significantly more reactive, than this parent complex. Notably, at pH 6.5, complex **C1**, with the ethylguanidinium pendant, was found to cleave UpNP at a rate 2.5 times faster than $[Cu(DPA)(OH_2)_3]^{2+}$, representing a 6-fold enhancement in rate compared to the background reaction (complexes **C2** and **C3** displayed similar reactivity to the parent DPA complex). At pH 7.4, complex **C3**, with a butylguanidinium pendant arm, achieved the fastest rate of cleavage, with over a 2-fold increase in rate compared to the background cyclization reaction, at both 25 and 37 °C. At pH 9, $[Cu(DPA)(OH_2)_3]^{2+}$, **C1** and the two tacn complexes did not accelerate UpNP cleavage above background levels. For **C1**, the drop in reactivity with increasing pH is more dramatic than for **C2** and **C3**. At pH 9, the reactivity of this complex is similar to that of the parent Cu−DPA complex. This finding is again consistent with the UV−vis−NIR spectrophotometric studies, which indicate that coordination of the guanidine pendant occurs following deprotonation. This process effectively deactivates the complex. In contrast, at pH 9, guanidine binding does not occur for

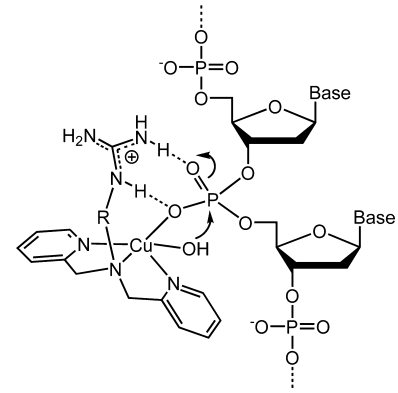

Figure 12. Plausible mode of interaction between the copper(II) complexes and DNA, leading to hydrolytic cleavage.

C2 and **C3**, and these complexes are in fact the most active of all of the agents tested in our study.

Notwithstanding the decreased reactivity of complex **C1** at high pH, the generally enhanced reactivity of the guanidine-bearing complexes compared to the parent Cu(II)−DPA complex can potentially be attributed to the guanidinium groups hydrogen-bonding to the uracil nucleobase, aiding substrate recognition and bringing the metal center in closer proximity to the phosphate ester linkage. Equally, the guanidinium groups may hydrogen-bond to the substrate's phosphate group, in a manner reminiscent of the arginine residue at the active site of alkaline phosphatase (Figure 1), in this way further activating the ribose phosphate to internal nucleophilic attack. The guanidinium moieties could also act as a ready source of exchangeable protons, facilitating proton transfer during the cleavage mechanism.

Cleavage of Plasmid DNA. Following the investigations with the model phosphate esters, we chose to examine the interaction of the complexes with supercoiled pBR 322 plasmid DNA, using gel electrophoresis, a well-established method for probing DNA scission by small metal complexes. Cleavage of the initially supercoiled form of pBR 322 (form I) produces an open, circular "relaxed" form (form II), which may be converted to a final linear form (form III) following cleavage of the second strand. In this study, the plasmid DNA was incubated with a large excess of complex **C1**, **C2**, or **C3** (*pseudo*-first-order conditions) for varying time intervals, under near physiological conditions (Figure 11 shows the data obtained at pH = 7.2 and T = 37°). Cleavage experiments were also performed with the nonfunctionalized "parent complex", $[Cu(DPA)(OH_2)_3]^{2+}$, to assess whether the guanidinium groups in **C1**−**C3** lead to enhanced DNA cleavage activity.

For each of the complexes, the intensity of the form I band was found to decrease with incubation time, accompanied by the appearance and intensification of a band corresponding to form II of the plasmid DNA (form III was not observed in any of our experiments). This clearly demonstrates that the complexes create single nicks in pBR 322 DNA. The extent of cleavage was found to be significantly greater for the complexes bearing guanidinium pendants. At pH = 7.2, a total of 84, 43, and 53% of the form I DNA initially present was converted to form II after 48 h for the reaction mixtures

containing **C1**, **C2**, and **C3**, respectively, compared to 22% for $[Cu(DPA)(OH_2)_3]^{2+}$. This enhanced DNA cleavage activity is reflected in the observed first-order rate constant (k_{obs}) of cleavage (Table 10), derived by fitting the decrease in the relative intensity of the form I band (or appearance of the form II band) to a first-order rate expression. The complexes are less efficient DNA cleavers than several copper(II) complexes reported in the literature, some of which exhibit first-order rate constants of over 2 orders of magnitude higher than previously reported systems.[21,30,41,54] It would seem that the optimal spacer distance for *cooperativity* of the guanidine in the hydrolysis of the phosphate ester bond is the ethyl linker (see Figure 12), however, this linker could also potentially enable the guanidine to coordinate to the metal center at higher pH values, slowing the rate of cleavage (*vide supra*).

Conclusion

A new series of copper(II) complexes of DPA derivatives featuring guanidinium pendants of varying lengths were synthesized. X-ray crystallography confirmed that the noncoordinating guanidinium groups can participate in charge-assisted hydrogen-bonding interactions with anionic molecules. Cleavage experiments performed with three different phosphate diester substrates revealed that the combination of a copper(II) center and guanidinium group in close proximity results in an enhanced ability to cleave plasmid DNA and, in some cases, an RNA mimic (UpNP). The complexes were, however, found to be less reactive than their nonfunctionalized parent complex in hydrolyzing the well-known activated phosphate diester, BNPP. Our results show that the trend in hydrolysis rates across a series of complexes in which the length of the guanidinium pendant is varied systematically, **C1**−**C3**, is not always preserved in going from, for example, an activated model phosphate ester, such as BNPP, to dsDNA or UpNP. This is also the case in going from the Cu−DPA complex to the complexes of the guanidinium derivatives. Hence, there is value in studying the reactions with a variety of phosphate ester types.

Acknowledgment. This work was supported by the Australian Research Council. M.J.B. was the recipient of an Australian Postgraduate Award and a Fulbright Fellowship.

Supporting Information Available: A CIF file. This material is available free of charge via the Internet at http://pubs.acs.org.

IC8004079

(54) Kobayashi, T.; Tobita, S.; Kobayashi, M.; Imajyo, T.; Chikira, M.; Yashiro, M.; Fujii, Y. *J. Inorg. Biochem.* **2007**, *101*, 348–361.